Design of a Novel Linkage for Electronic Parking Brake Transmission Systems

DESIGN OF A NOVEL LINKAGE FOR ELECTRONIC PARKING BRAKE TRANSMISSION SYSTEMS

Giuseppe Quaglia[1,†,*], Fortunato Pepe[2,†], Lorenzo Toccaceli[1,†], Giovanni Colucci[1,†,]**

[1]Politecnico di Torino, Torino, Italy
[2]SKF Industrie, Airasca, Italy

ABSTRACT

The paper presents a novel mechanical transmission for pulling-cable Electronic Parking Brakes. The system is interposed between the brake electric actuator and the brake pads, and it exploits a 2-dof planar linkage to provide the requested brake force and ensure the correct vehicle standstill. The paper describes the working principles and main component of the adopted architecture, and compares it with the EPB state of the art. Thereafter, the paper focuses on the system requirements and consequent functional design. A first prototype of the presented mechanical transmission is then presented to discuss the role of a mechanical engagement within the system to ensure its proper behaviour. In conclusion, the EPB drive motor assessment is discussed on the basis of a simplified drive chain dynamic model.

Keywords: Electric Parking Brake, Planar Linkage, Cable Puller EPB, Mechanism Design

NOMENCLATURE

Roman letters

$< \hat{i}, \hat{j}, \hat{k} >$	Fixed reference frame
$< \hat{u}, \hat{v}, \hat{w} >$	Mobile reference frame
X, Y	Position of respectively cursor A and cursor U along $\hat{i}$ axis of $< \hat{i}, \hat{j}, \hat{k} >$ [m]
x, y	Position of respectively cursor A and cursor U along $\hat{u}$ axis of $< \hat{u}, \hat{v}, \hat{w} >$ [m]

Greek letters

τ	Linkage transmission ratio during the rotating mode

Superscripts and subscripts

i, f	Initial and final configuration of the linkage rotating mode
min, max, min	Minimum, intermediate and maximum pulling cable stroke

1. INTRODUCTION

In the past years, new trends and requests coming from the automotive market have led to the establishment of the EPB (Electronic Parking Brake) system as an effective and reliable solution. Pursuing the general trend of converting classical mechanical operations into electrical ones, Electric Parking Brake devices were first introduced at the beginning of the 21st century to increase the passenger's comfort and security [1].

The EPB main functionality consists of driving the vehicle rear brake system to guarantee its correct stationing, but it also provides additional functionalities, e.g. start and stop assist, hill assist, and emergency braking. The standard EPB system consists of a control element, e.g. an electrical switch, positioned in the vehicle cockpit, that activates the EPB employing an ECU (Electrical Control Unit) [2].

Within the EPB market, a main distinction is usually made depending on how the system is coupled with the brake calipers, resulting into the two categories of pulling-cable devices and integrated calipers, as shown in Fig. 1. In the first case [3–7], the electronic parking brake is coupled with the brake system using a Bowden cable, with the potential advantage of positioning the device in an unused area of the vehicle and without strict compactness restrictions. Nevertheless, the limited stiffness of the cable and the related friction phenomena that affect its motion cause a worse dynamic response and a worse efficiency than the integrated calipers solution. The latter case [2, 8–10], instead, requires an electronic parking brake device for each axle shaft, and is affected by dimension limitations. However, they are often marked by a higher efficiency and lower value of required input power [11].

Regardless of its classification, the EPB standard mechanical layout consists of an electric drive motor, a reduction gearing, and a motion conversion unit, from rotatory to linear [1, 12]. Fig. 2(a) shows the standard mechanical layout of a cable-puller EPB. The need for a reduction unit arises from the required brake force versus caliper stroke characteristics, which monotonically increase to final clamping values that a direct motor-caliper coupling would not be able to fulfill. The motion conversion unit, instead, is typically carried out by a spindle-nut system, a ball screw drive, or similar.

In addition to these static apply design requirements, the correct vehicle stationing needs the reach and subsequent holding of a desired brake caliper stroke, even when the drive motor is turned

[†]Joint first authors
[*]Corresponding author: giuseppe.quaglia@polito.it, giovanni_colucci@polito.it

Documentation for `asmeconf.cls`: Version 1.36, February 21, 2024.

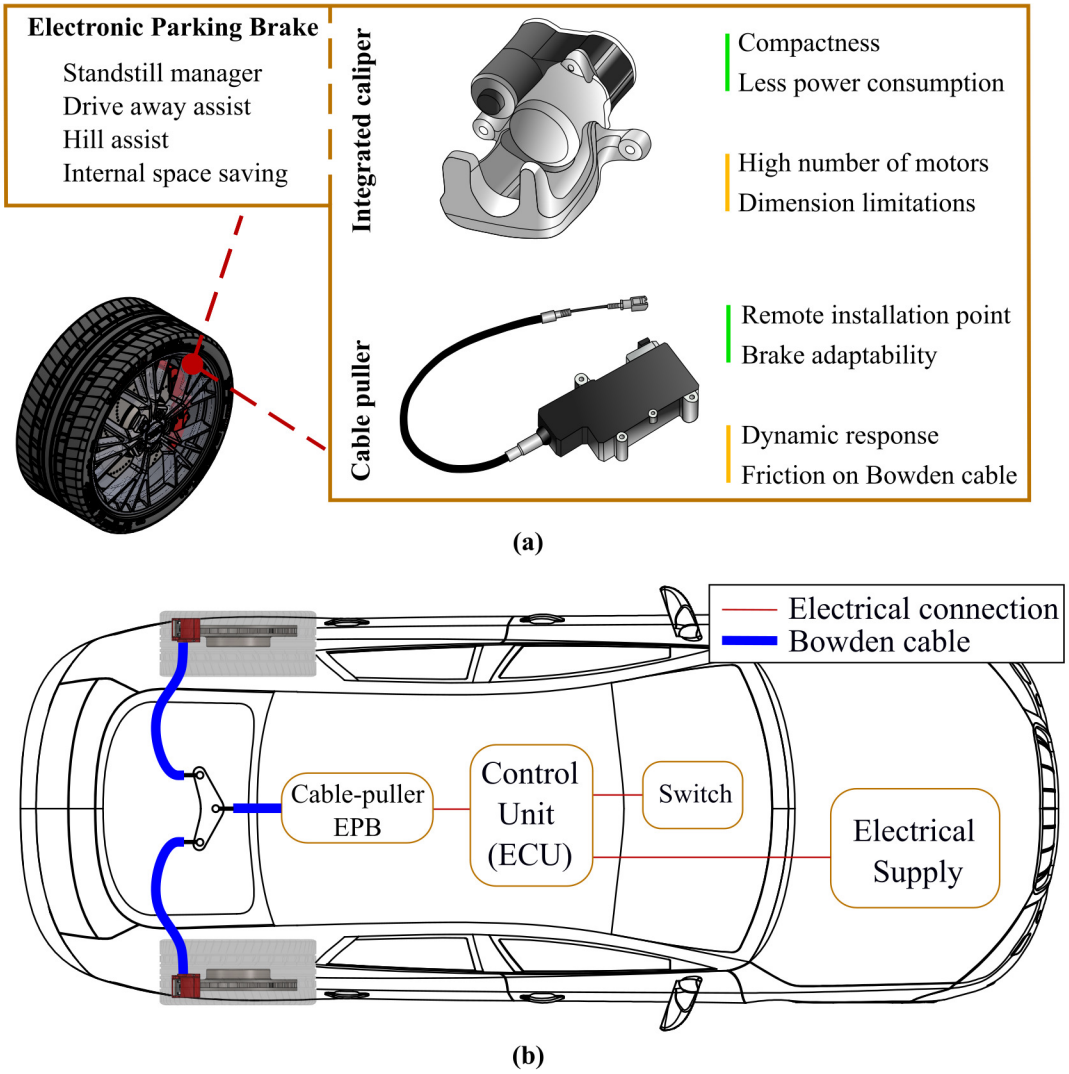

FIGURE 1: (a) EPB main functionalities and typologies. (b) Standard cable puller EPB integrated system [1].

off. Thus, the caliper motion irreversibility plays a key role within the static apply design requirements. It is worth noticing the use of a screw drive gear acts as a conversion unit that also guarantees the motion irreversibility, which justifies its wide and spread deployment among the electronic parking brake manufacturers [11].

Notwithstanding their specific mechanical layout, all the cited commercial EPB solutions are marked by a constant value of the transmission ratio. Thus, by neglecting eventual mechanical dissipative phenomena, the brake force characteristics can be easily converted into the required drive force/torque by means of a constant factor. In this regard, the typical brake force behavior is schematized in Fig. 3 as a function of the caliper stroke, where two distinguished phases, respectively the approaching (pink area) and clamping phase (blue area), are outlined [12, 13]. When the EPB is not enabled, integrated return springs keep the brake calipers in the rest position. Thus, in what is defined as the approaching phase (i.e. the pink area of the graph), the required brake force is mainly influenced by the return spring elastic force and, eventually, by friction (e.g. between cable and sleeve for a cable-puller EPB). Then, due to the pads-disk contact, the characteristics significantly change its slope, entering into the actual clamping phase (blue area). The significant order-of-magnitude jump between the approaching and clamping phases may clearly lead to the design of an oversized drive chain, for it should guarantee the reach of the required maximum brake force. This aspect suggests the design of a variable transmission ratio system which can help in reducing the drive motor size.

Fig. 3 also depicts the brake wear effect on the force characteristics, which results in the shift of bite point A; albeit the clamping phase curve slope, which depends mainly on the pad thickness and temperature [13], can be assumed as constant. It is worth underlining the bite point A, i.e. the point which marks the substantial curve slope change, is not easy to determine a priori due to the characteristics of the specific braking system and also due to the brake pads wear phenomena [13]. Besides, the phase transition, here simplified with a clear and marked slope change, is often not that concentrated, and its mathematical representation is a nontrivial concern [12]. Nevertheless, this additional matter also suggests the design of a transmission chain that automatically

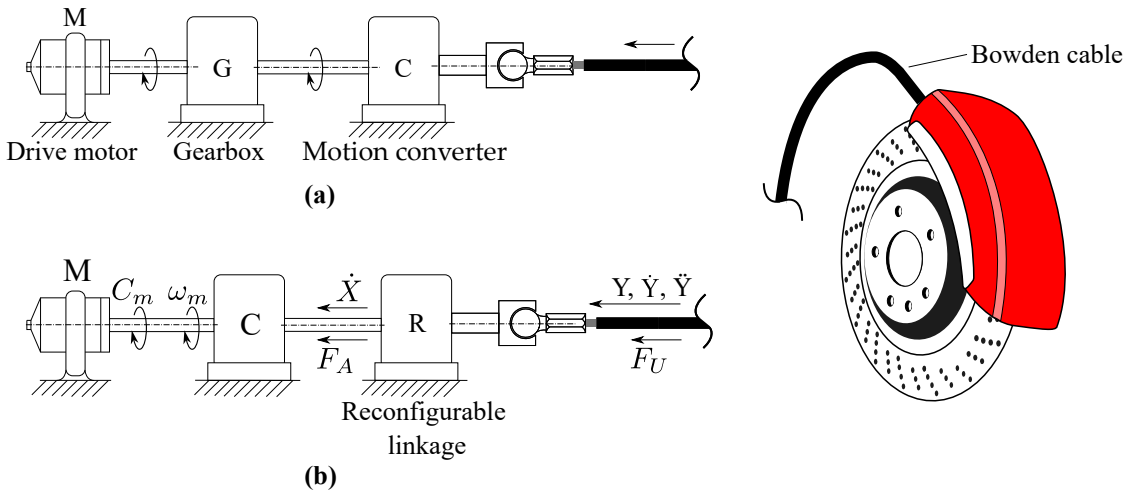

FIGURE 2: (a) Cable-puller EPB mechanical layout. (b) EPB.QI layout.

recognizes the phase transition area, thus adapting to its natural and inevitable shift.

By considering all the key features of a modern EPB trasmission system above described, the paper main objective regards the functional design of a two degrees-of-freedom planar linkage for cable puller EPB transmission systems. This system, named EPB.QI, integrates all the cited static apply requirements, specifically by introducing a variable transmission ratio during the clamping phase and also by guaranteeing the motion irreversibility without exploiting friction phenomena. Besides, in order to take into account the bite point A shifting during working conditions, the EPB.QI linkage kinematics is not a priori imposed, thus exploiting an additional sub-system, here named mechanical engagement, that allows the automatic bite point detection.

This paper is an extended work of what was already presented by the authors in the "6th IFToMM International Conference on Mechanisms, Transmissions, and Applications (MetrApp2023)" [14]. As main contributions of the present paper, sections 2 and 3 present a few functional design insights, while section 4 describes the mechanical engagement subsystem that allows the EPB.QI linkage mode switching and shows the EPB.QI preliminary prototyping. At last, toward the integration of the EPB.QI with its related drive chain, in section 5 the electric drive motor assesment methodology is discussed on the basis of a simplified dynamic drive chain model.

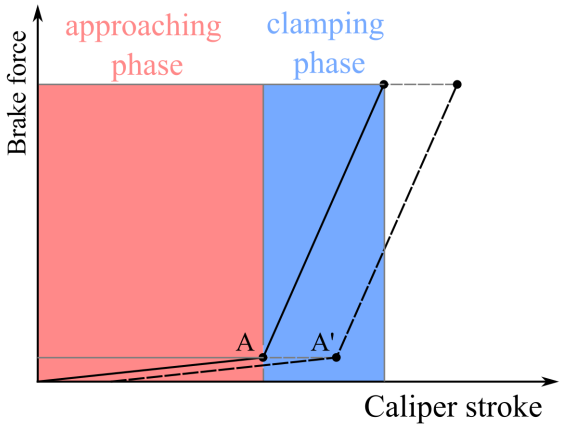

FIGURE 3: Simplified brake force characteristic under variable mounting and wear conditions. The approaching and clamping areas are referred to the first condition (continuous line).

2. THE EPB.QI TRANSMISSION SYSTEM

The EPB.QI mainly consists of a motion conversion unit and a planar 2-dof linkage. A schematic representation of EPB.QI is depicted in Fig. 2(b), where the motion conversion unit is positioned upstream of the EPB.QI that acts as a force amplifier with a variable transmission ratio.

Figure 4 shows a detailed representation of the EPB.QI linkage, where the relevant geometrical parameters are also made explicit. The three main components of the linkage, namely cursors A, U, and the mobile frame, are mounted on linear slides that guide the translational motion. A hinge joint connects the mobile frame to a ternary link, named BDE, whose initial orientation with respect to the mobile frame is described by angle $\Delta\alpha$ and it is imposed by a mechanical end stop. F_A and F_U are respectively the drive and resistive force acting on slider A and U. The last main component of EPB.QI prototype is shown in Fig. 4 under the name of a generic mechanical engagement. Even though it will be explained hereafter, it is worth underlining this component is fixed to the mobile frame and it interacts with the fixed frame.

2.1 Design Requirements

Basing on what discussed above, the design of an Electronic Parking Brake transmission system relies on the following static and dynamic apply requirements:

- The total cable stroke Y_t. This value depends on the brake architecture and model, along with the level of brake wear and backlash. The EPB must typically guarantee a total stroke Y_t ranging between a minimum and a maximum value.

- The exerted pulling force F_U, described as a function of the cable stroke $F_U = F_U(Y)$. Fig. 5 shows the $F_U(Y)$ behavior,

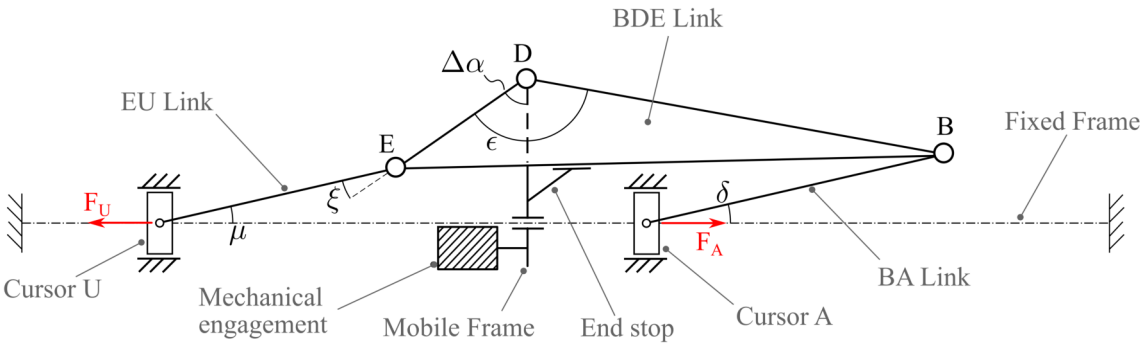

FIGURE 4: EPB.QI two degrees of freedom linkage, schematic representation.

where $F_{U,A}$ is the clamping force at the bite point A and $F_{U,M}$ is the maximum required clamping force.

- The total brake actuation time T, that is often imposed by the desired vehicle performance.
- The application current i_m, that is required from the electric motor, and it is often limited by the motor driver.
- The irreversibility of motion, both in initial ($Y = 0$) and final ($Y = Y_f$) configuration of the EPB device, to prevent sudden activation of the brake or its undesirable release.

It is worth underlining the need for an adjustable cable stroke depends on several concerns that occur during the EPB functioning. First, the approaching phase is marked by the compensation of the eventual backlash that is present in the kinematic chain. In addition, the desired $F_{U,M}$ that must be reached (and maintained) by the EPB depends on vehicle specifications, and it may correspond to different values of cable stroke depending on the brake pads wear level.
In summary, the following values are design requirements uniquely imposed by the brake system whom the EPB has to drive:

- $F_{U,A}$, i.e. the actuation force corresponding to the bite point A. Depending on the brake backlash and pad wear level, it may change during the EPB life cycle.
- $F_{U,M}$, i.e. the maximum actuation force that guarantees the correct vehicle stationing.
- ΔY, i.e. the cable stroke during the clamping phase, that is mainly related to the braking system stiffness.

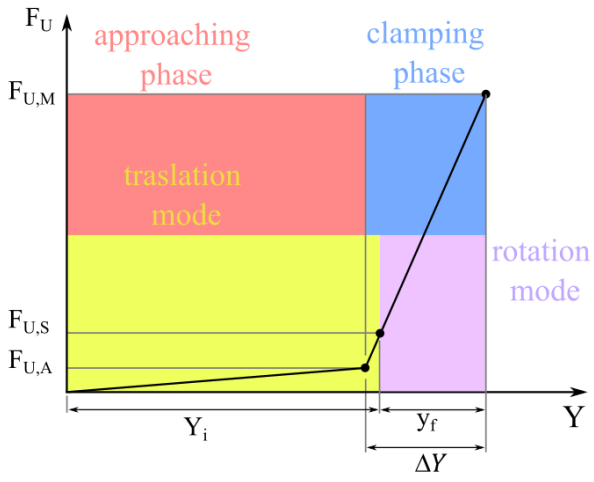

FIGURE 5: Pulling force vs. cable stroke characteristics. The yellow and pink areas represent the translation and rotation EPB.QI working modes. Please notice the mode transition happens at a value of the pulling force that is above the bite point.

2.2 EPB.QI working principle

Even though the EPB.QI planar linkage is marked by two degrees of freedom (dofs), i.e. the translation of the mobile frame and the relative rotation of BDE ternary link with respect to (w.r.t.) the mobile frame itself, the EPB.QI functioning relies on the basic idea of exploiting these two dofs separately (see Fig. 5 and Fig. 6).
The first working mode, namely the translation mode, corresponds to a $Y - F_U$ graph area with a relatively large cable stroke but low pulling forces. As the name suggests, in this modality the BDE link rotation is averted, i.e. the relative motion between cursor A and U is denied, and the entire EPB.QI translates with respect to the fixed frame; acting as a rigid body and without introducing any transmission ratio within the transmission kinematics (Fig. 6(a)). When the pulling force characteristics is near the bite point A, the desired behavior of the EPB.QI expects the lock of the mobile frame. As a result, the prosecution of cursor A motion provokes the relative rotation of BDE w.r.t. the mobile frame. In this fashion, the transmission system acts as an articulated mechanism within the $< \hat{i}, \hat{j} >$ plane.
It is worth underlining how the mode transition, from translation mode to rotation one, does not happen exactly at the bite point, but at a value of pulling force $F_{U,S} > F_{U,A}$. This behavior, together with the BDE rotation lock during the approaching mode and the mobile frame lock during the rotation mode, is entirely demanded to the mechanical engagement, which is here not represented for simplification purposes and is described on section 4.
In Fig. 6 a representation of what explained above is presented in form of a schematic drawing, with additional information about

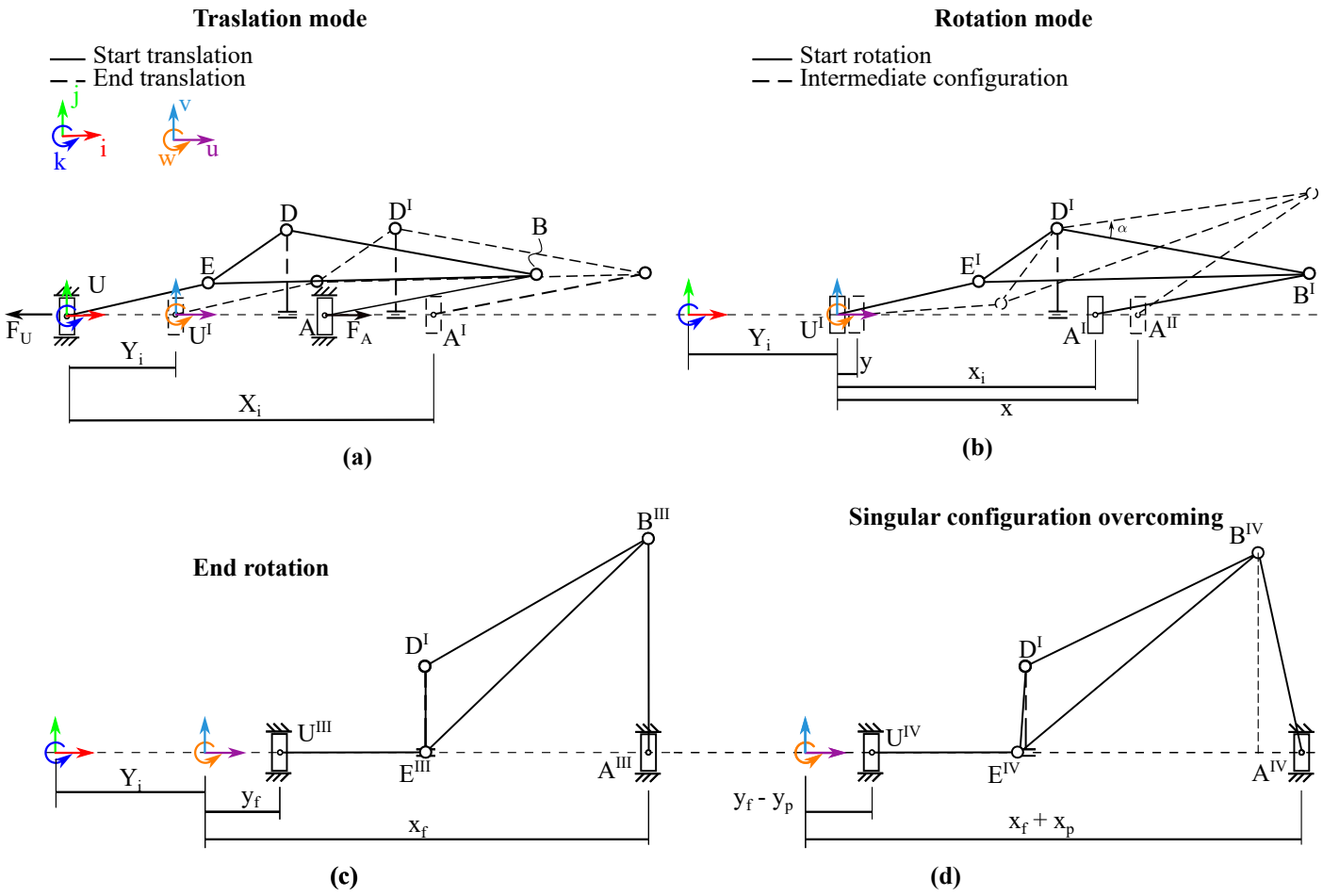

FIGURE 6: EPB.QI working modes. The mechanical engagement is not represented for simplification purposes. (a) Translation mode, (b) Rotation mode, (c) End configuration of the rotation mode, (d) Singular configuration overcoming to guarantee the motion irreversibility.

reference frames and the main parameters of each mode. The $< \hat{i}, \hat{j}, \hat{k} >$ is the fixed reference frame, positioned in the initial position of cursor U during the translation mode. On the other hand, $< \hat{u}, \hat{v}, \hat{w} >$ is a mobile-frame-attached reference frame, thus it stops during the rotation mode.

Another interesting aspect of the EPB.QI architecture lies in the attainment of the motion irreversibility of the pulling cable, which is fixed to cursor U, thanks to the overcoming of a singular configuration, that is shown in Fig. 6(c) and Fig. 6(d). Regarding this choice, a possible drawback could lie in the value of y_p, which quantifies the backward motion of cursor U during the cited overcoming. This issue would turn into a cable release, though minimal. To avoid this behavior, the functional design must guarantee the motion irreversibility with a negligible backward motion of cursor U.

3. LINKAGE DESIGN AND TRANSMISSION RATIO EVALUATION

Within the present section, the functional design of the electronic parking brake as a function of the cited requirements is presented. The kinematic variables of the system are the following (Fig. 6):

- X, Y Position of A and U along $\hat{i}$ axis.

- x, y Position of A and U along $\hat{u}$ axis.

Using the subscript $[]_{i,f}$ to respectively refer to the starting and final configuration of the rotating mode, the total stroke Y_t can be described as follows:

$$Y_t = Y_i + y_f \tag{1}$$

While the connection between the design requirements and the Y_i value is straightforward, the evaluation of the displacement of cursor U w.r.t. $< \hat{u}, \hat{v}, \hat{w} >$ during the rotation phase, i.e. $y = y(x)$, depends on the geometric parameters reported in Table 1 and shown in Fig. 4.

Thus, the design procedure can be performed in terms of several values, that are hereinafter described.

First, the overall linkage encumbrance is defined within the $< \hat{i}, \hat{j} >$ plane with V_t (vertical) and H_t (horizontal). While it is straightforward how $H_t = Y_i + H_{rot.\,mode}$, where the latter term represents the horizontal emcumbrance of the system during the rotation mode; V_t may be affected by the height z_D or the position of B^{IV} point. In addition, the linkage kinematics is studied in terms of cable stroke characteristics $y = y(x)$ and

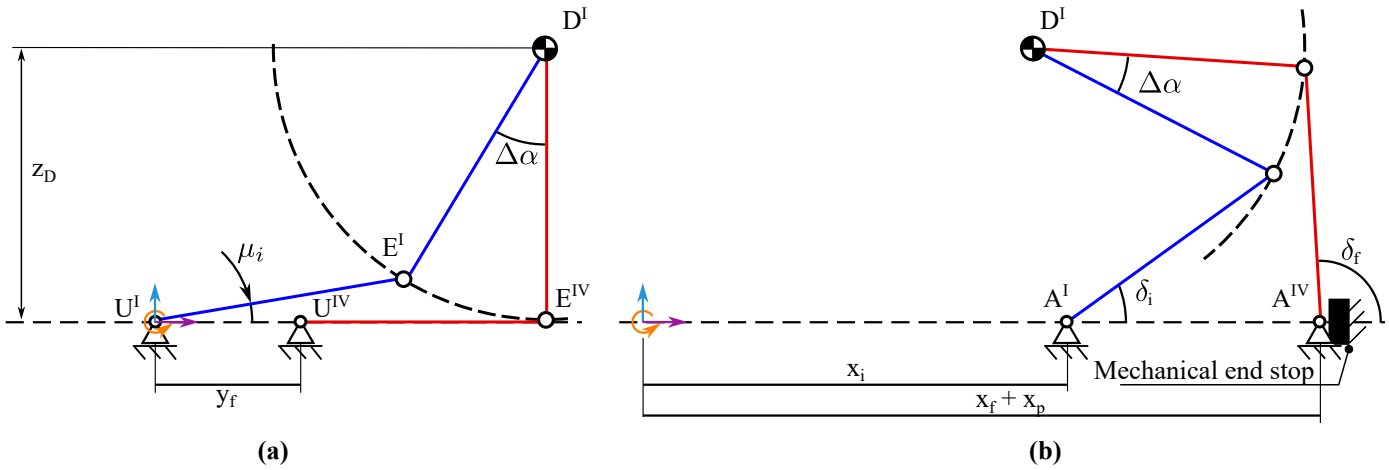

FIGURE 7: EPB.QI design preliminary assumptions. (a) $\delta_f = 0$, (b) $\delta_f > 90$ deg. A mechanical end stop is used to keep cursor in A in the correct position during the vehicle parking, thus the brake caliper motion irreversibility does nor rely in friction phenomena.

TABLE 1: EPB.QI functional design parameters.

Name	Description
AB, EU	Length of AB and EU links
DE, DB	Characteristic lengths of ternary link BDE
z_D	Offset of D along $\hat{j}$
$\delta(x)$	Pressure angle of AB
$\mu(x)$	Pressure angle of EU
ϵ	Angle between DE and DB direction of DBE
$\xi(x)$	Angle between DE and EU link

transmission ratio, that is defined as follows:

$$\tau(x) = \frac{dy(x)}{dx} \tag{2}$$

By neglecting friction phenomena, the quasi-static behavior of the actuation force during the rotation phase can be computed as:

$$F_A = \tau(x)\, F_U(x) \tag{3}$$

The functional design here described can be simplified on the strength of preliminary choices, that also address relevant technological issues. In this fashion, the first design choice was already presented in Fig. 6(c), even though not explicated, and it concerns the pressure angle of EU in the end configuration of the rotation phase. This value is imposed to (see Fig. 7(a)):

$$\mu(x = x_f) = \mu_f = 0\, deg \tag{4}$$

to maximize the pulling force transmitted to cursor U when the required F_U reaches the highest value $F_{U,M}$. This choice also leads to the following results:

$$z_D = DE \tag{5a}$$

$$\xi_f = 90\, deg \tag{5b}$$

Please notice how the following simplification was done:

$$y_p \approx 0 \tag{6}$$

Then, the final value of the pressure angle of BA is imposed as (see Fig. 7(b)):

$$\delta(x = x_f) = \delta_f > 90\, deg \tag{7}$$

to guarantee the irreversibility of motion by means of the joint action of the singular configuration overcoming and a mechanical end stop.
Finally, additional choices may be done regarding practical and technological issues. Among them, the following remarks significantly influence the linkage design:

- A minimal length of BA and EU link must be respected. In this regard, a value of 15mm was chosen by the authors for the EPB.QI design.
- To compact the transmission system along the $\hat{k}$ axis, all the sliders may be positioned on the same linear guide. In this fashion, the mechanical interference during the rotation between all the components must be avoided.

3.1 Functional Design methodology

As a possible design methodology, Fig. 8 shows a block diagram that addresses the problem by treating the linkage as two separate slider-crank mechanisms that are coupled by means of the fixed angle ϵ. Regarding the first block, the method considers the lengths DE and EU as design input, while the second block relies on the values δ_i and a, b.
In more details, the DE-EU linkage is at first designed by considering the mean cable stroke value $y_{f,int}$ over the range $y_f = [y_{f,min}, y_{f,max}]$ and imposing both Eqn. 4 and Eqn. 5 (b). In this fashion, the cable stroke $y_{f,int}$ and DE link length are described by the following equations:

$$y_{f,int} = DE \cdot \sin(\Delta\alpha) + EU \cdot (\sin(\Delta\alpha + \xi_i) - 1) \tag{8a}$$

$$DE = \frac{EU \cdot \cos(\Delta\alpha + \xi_i)}{1 - \cos\Delta\alpha} \tag{8b}$$

that are used to compute $\Delta\alpha$ and μ_i as function of the input values DE and EU. Thus, in a similar manner,the DB-BA linkage design

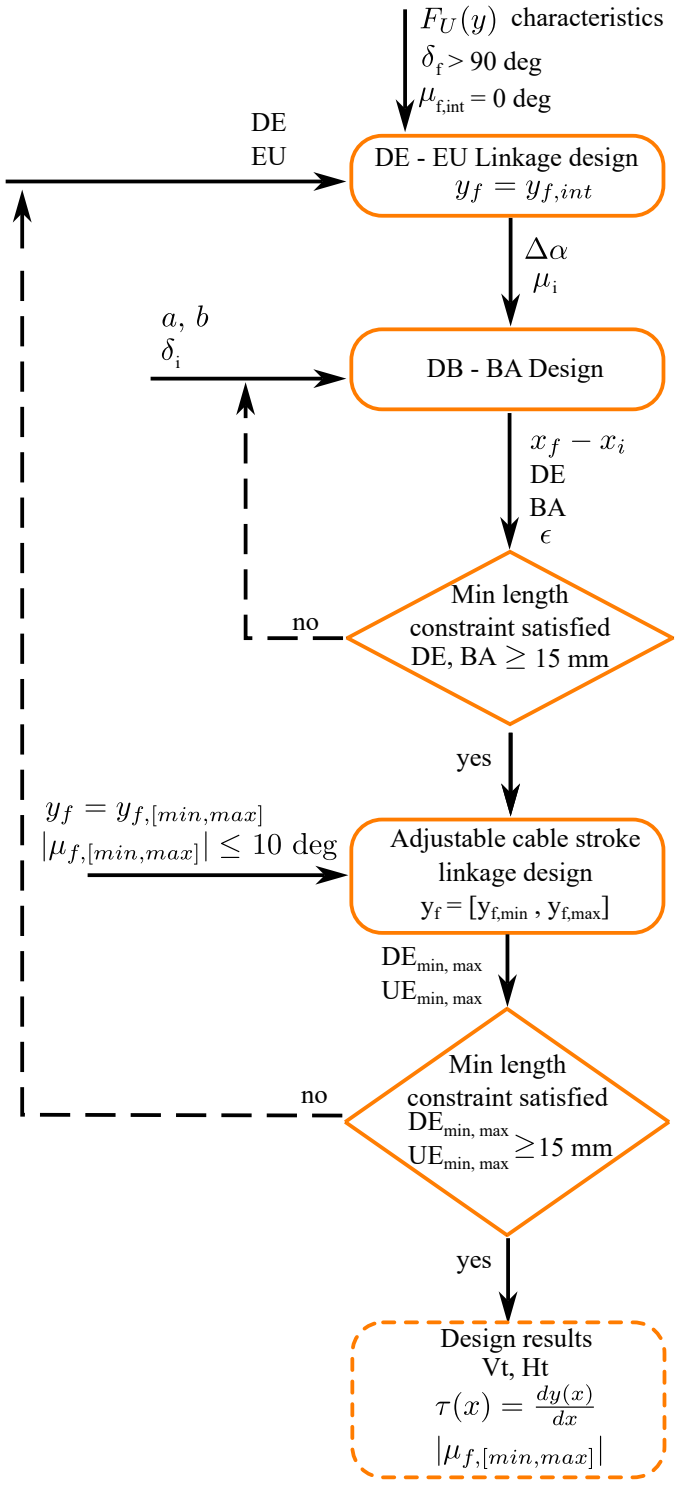

FIGURE 8: Functional design methodology block diagram.

can be done by means of the following statements:

$$DE = DB \cdot \cos(\epsilon) + BA \cdot \sin(\delta_f) \tag{9}$$

$$DE = DB \cdot \cos(\epsilon - \Delta\alpha) + BA \cdot \sin(\delta_i) \tag{10}$$

$$x_f - x_i = DB \cdot (\sin(\epsilon) - \sin(\epsilon - \Delta\alpha)) + - BA \cdot (\cos(\delta_f) - \cos(\delta_i)) \tag{11}$$

where the cursor A stroke during the rotation phase, namely $x_f - x_i$ is defined by considering the energy balance of the mechanism during the rotation phase, that is:

$$P_{in} = P_{out} \rightarrow F_A \frac{dx}{dt} = F_U \frac{dy}{dt} \tag{12}$$

that leads to:

$$\int_{x_i}^{x_f} F_A dx = \int_0^{y_f} (F_{U,S} + Ky) dy \tag{13}$$

where

$$K = \frac{F_{U,M} - F_{U,S}}{y_f} \tag{14}$$

represents the slope of the pulling force characteristics during the clamping phase (Fig. 5). The above equation can be rewritten by means of the integral mean value $\bar{F}_A$:

$$\bar{F}_A (x_f - x_i) = F_{U,S}\, y_f + \frac{1}{2} K y_f^2 \tag{15}$$

which easily leads to:

$$\frac{x_f - x_i}{y_f} = \frac{1 + \frac{F_{U,M}}{F_{U,S}}}{2\,\frac{\bar{F}_A}{F_{U,S}}} \tag{16}$$

Now considering the two values a and b, defined as:

$$a = \frac{F_{U,M}}{F_{U,S}} \tag{17a}$$

$$b = \frac{\bar{F}_A}{F_{U,S}} \tag{17b}$$

Eqn. 16 can be written as follows:

$$\frac{x_f - x_i}{y_f} = \frac{1 + a}{2\,b} \tag{18}$$

Once the EPB.QI linkage design is completed for the mean cursor U stroke value $y_{f,int}$, the procedure could proceed or be stopped depending on the value of DE and BA link lengths, for which a minimum value of 15 mm is imposed for practical and technological concerns.

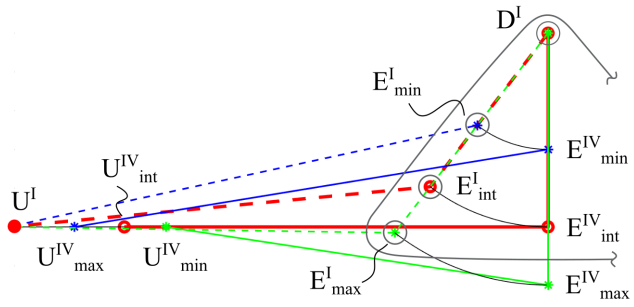

FIGURE 9: Cable stroke adjustment through $D^I E^I$ variation. Please notice this methodology does not affect the DB-BA drive slider crank mechanism. The subscripts $[]_{min, int, max}$ are respectively related to the minimum, intermediate and maximum EPB.QI cable stroke.

3.2 Adjustable cable stroke

The adjustable cable stroke linkage design represents another main aspect of the design methodology. As cited in section 2.1 about the design requirements of EPB.QI, a cable puller EPB must guarantee an adjustable cable stroke due to the application of the system to several and different vehicle brake architectures. Nevertheless, it is worth remarking that the cable stroke is usually a design requirement imposed by the end-user, thus it is defined during the design process and it is not changed when the EPB is operating. Within the paper, the term "cable stroke adjusting" is thus used to refer to a modification of the cable stroke that is done before the EPB installation on the vehicle.

Fig. 9 shows how this problem may be addressed by means of the DE-EU linkage adjustment. This method is based on a variable length of EU link and of its connection point on the ternary link BDE. Thanks to this approach, the rotating mode stroke can be changed inside the range $[y_{f,min}, y_{f,max}]$ without changing the initial point of U link, i.e. U^I, and also without any modification on the driving linkage DB-BA.

Nonetheless, this stroke adjusting approach produces the unwanted effect of changing the final value of the pressure angle μ_f, that increases the vertical component of the force transmitted by slider U on the prismatic joint. To minimize this effect, the suggested approach is to still impose $\mu_f = 0$ for the intermediate value of stroke $y_{f,int}$, then to keep under control the maximum value $max[|\mu_{f,min}|, |\mu_{f,max}|]$. The variable cable stroke design thus represents the last process block depicted in Fig. 8 and substantially consists in the reproduction of what done for DE-EU linkage with $y_{f,int}$ but now considering the two boundary values $y_{f,min}$ and $y_{f,max}$. In this case $\Delta\alpha$ is nonetheless imposed, as well as the direction along with the two points $E_{min,max}{}^I$ lie.

It is also worth noticing how the value of the link length DE follows the behavior of the stroke y_f, i.e. if the stroke is reduced, the link length DE reduces too. Link length EU, instead, follows the opposite behavior.

3.3 Design results

The proposed design method in Fig. 8 can be used to compute and compare several solution sets, in terms of geometries, overall dimensions and transmission ratio. Among them, Table 2 shows a possible solution for a cable stroke range of $y_f = [10, 20]$ mm, thus $y_{f,int} = 15$ mm. The total dimension along $\hat{i}$ axis is measured as the sum of Y_i, which has here the value of 20 mm, and the horizontal encumbrance of EPB.QI during the rotating phase. The pressure angle of link EU is kept within the range $[-10, 10]$ deg, while the most critical value of EU is related to the maximum stroke and it corresponds to 61 mm. On the other hand, $DE_{y_f=y_{f,min}} = 17$ mm, which is nevertheless a reasonable value for executive design concerns.

Regarding the transmission ratio behavior $\tau(x)$, its monotone decreasing characteristics is depicted in Fig. 10, where it is evident how it each curve goes when it gets closer to the singular configuration. Since the transmission ratio value during the translation mode is evidently unitary, for the EPB.QI is just translating along the $\hat{i}$ axis, there is a sudden drop-down of the curve when the system switches from translating to rotating mode. This causes a velocity discontinuity of the pulling cable, especially when the cable stroke is near its minimum value. Nevertheless, according to the authors, a velocity discontinuity of the cable stroke doesn't represent a possible critical drawback for the correct functioning of a cable puller EPB, since the actual brake has yet to occur.

TABLE 2: Design methodology results, $y_f = [10, 20]$ mm.

$y_{f,int} = 15$ mm	$y_{f,min} = 10$ mm	$y_{f,max} = 20$ mm
DE / $y_{f,int} = 1.67$	DE / $y_{f,min} = 1.7$	DE / $y_{f,max} = 1.6$
EU / $y_{f,int} = 3.67$	EU / $y_{f,min} = 6.1$	EU / $y_{f,max} = 2.55$
$\mu_{f,int} = 0$ deg	$\mu_{f,min} = 7$ deg	$\mu_{f,max} = -8$ deg
$\epsilon = 120$ deg		
DB / $y_{f,int} = 6.4$		
BA / $y_{f,int} = 4.87$		
V_t / $y_{f,int} = 4.93$		
H_t / $y_{f,int} = 1.3 + 4.93 = 6.26$		

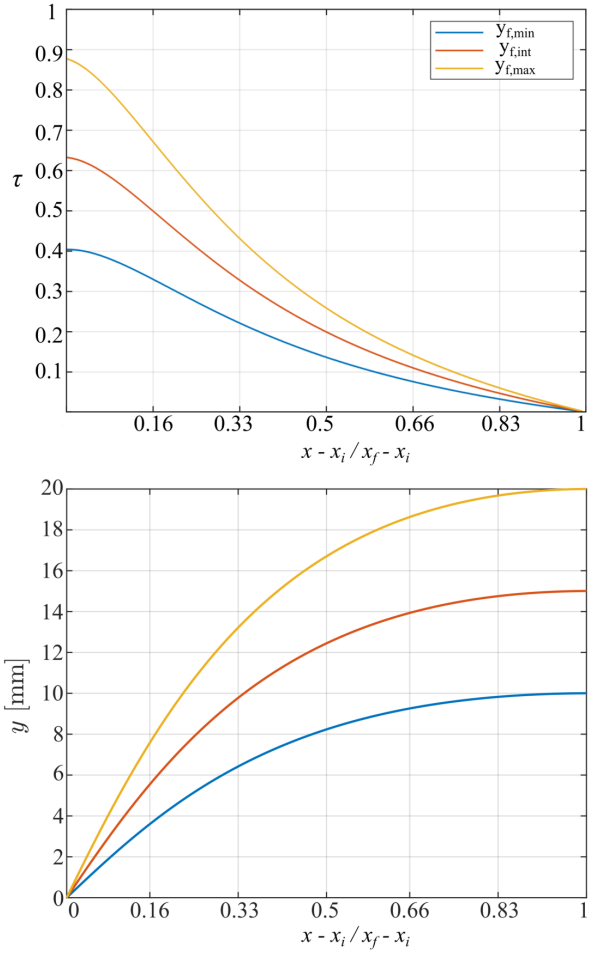

FIGURE 10: Transmission ratio and cable stroke characteristics regarding the solution set of Table 2. x_i, x_f are defined accordingly to Fig. 6.

4. ENGAGEMENT AND DISENGAGEMENT CONSIDERATIONS

As previously mentioned, the EPB.QI transmission system includes a planar linkage whose 2-dofs are meant to be used separately to make the EPB.QI work as a translating or rotating mechanism. Nevertheless, if its kinematics is not imposed, the system itself would not be capable of changing its behavior in correspondence with the desired value of brake force $F_{U,S}$. Therefore, within the present section, the additional components that are in charge of making the system work as desired, also imposing the transition at the exact value $F_{U,S}$ are discussed.
First, during the translation mode, if no additional components are added, the ternary link BDE tends to rotate counter clock-wise if that motion is not prevented. By observing Fig. 11, indeed, since $F_U = F_A$ during this modality, the net torque acting on BDE with respect to D is equal to:

$$\sum_i M_{D\,i} = F_{BA}\, DB\, sin(\delta_i + \pi/2 - (\epsilon - \Delta\alpha)) + \\ - F_{EU}\, DE\, sin(\pi/2 - \mu_i - \Delta\alpha) \tag{19}$$

that, by substituting the resulting values above presented, gives back a positive (counter clock-wise) net torque. To avoid this behavior, a generic clockwise torque must be added within the mechanism to avoid the relative rotation in D until $F_{U,S}$ is reached. Among all the possible technical solutions, Fig. 12(a) and (b) present the implementation of a traction spring connected between C on the mobile frame and P on BDE. As a main benefit of this choice, the line joining the two fixing points, i.e. $\overline{CP}$, overtakes the hinge joint D during the rotation, thus resulting in a clockwise torque during the mode transition and a consecutive reduction down to null and even negative torque values in the final part of the rotation mode.
As alternative, Fig. 12(c) and (d) schematize the use of a flat spring acting between the mobile frame and slider A, here modeled as a concentrated hinge joint with a torque spring. By referring the force acting on links BA and EU to respectively F_A and F_U, it is possible to rewrite Equation 19 to calculate the value of maximum attractive force $F_{0,max}$ that is needed to guarantee the mode transition at the desired value of cable pulling force $F_{A,S}$ by implementing the flat spring option:

$$\sum M_D = (F_A - F_0)\, \frac{DB\, sin(\delta_i + \pi/2 - \epsilon + \Delta\alpha)}{cos(\delta_i} + \\ - F_U\, \frac{DE\, sin(\pi/2 - \mu_i - \Delta\alpha)}{cos(\mu_i} \tag{20}$$

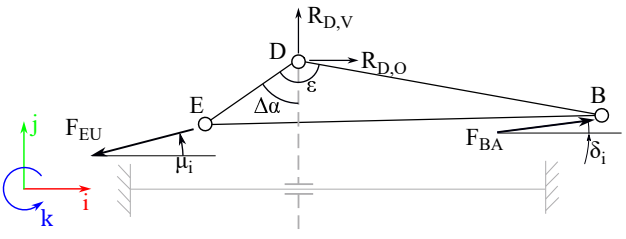

FIGURE 11: Ternary link BDE free body diagram during the translation mode. The mechanical engagement is yet not present.

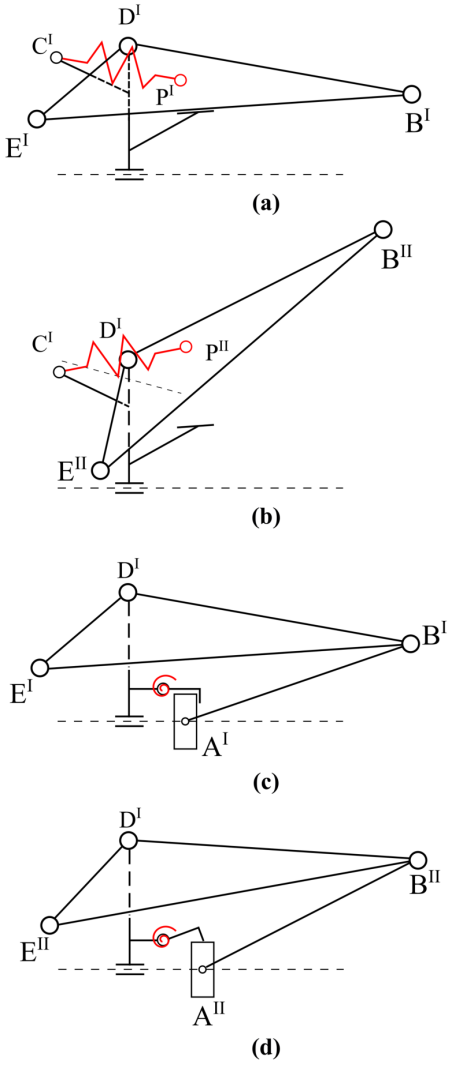

FIGURE 12: Mechanical engagement example for the mode switch. (a) and (b) traction spring, $y = 0$ and $y > 0$, (c) and (d) flat spring, $y = 0$ and $y > 0$.

that leads to:

$$F_{0,max} = F_{U,S}\left(1 - \frac{DE\, cos(\delta_i}{DB\, cos(\mu_i}\, \frac{sin(\pi/2 - \mu_i - \Delta\alpha)}{sin(\delta_i + \pi/2 - \epsilon + \Delta\alpha)}\right) \tag{21}$$

4.1 Mobile frame locking system

Regarding the mobile frame, the internal support force $R_{D,O}$, acting on BDE in Fig. 11, is evidently transmitted to the mobile frame through the hinge joint D. This force, now acting on the mobile frame, is concordant with $\hat{\imath}$ during the translation mode, but, since $\tau < 1$ during the rotation mode, it is straightforward to verify that, in pseudo-static condition:

$$R_{D,O}^{mobile\,frame}(x) = \frac{F_{BA}}{cos(\delta_i)} - \frac{F_E U}{cos(\mu_i)} = F_A - F_U < 0 \tag{22}$$

Since the EPB.QI functioning foresees the mobile frame lock during the rotation mode, this behavior can be obtained by exploiting

this $R_{D,O}^{mobile\,frame}$ change in sign. Thus, the mechanical engagement may also include a free-wheel-like mechanism [15, 16], acting as a mechanical diode to suppress the mobile frame backward motion during the rotation mode. This kind of system takes generally the advantage of roller, micro ratchet, modular ratchet, or sprag mechanisms to obtain a One-Way Clutch (OWC). In a similar fashion, but now applied to a linear motion instead of a rotational one, the closure of a linear OWC may rely on friction phenomena between the sliding contact surfaces or alternatively on the engagement of a ratchet mechanism. Among them, the sprag OWC has the main advantage of transmitting higher forces with lower drag, even though they are historically more expensive [15]. The evaluation of a linear OWC for the EPB.QI transmission system is not addressed within this paper but, nonetheless, the state of the art of these systems may lead to the design of a sprag-based one-way linear clutch.
Fig. 13 depicts the resulting design of an EPB.QI equipped with a mechanical engagement consisting of flat springs and ratchet-based OWC. The motion irreversibility is obtained by means of a mechanical end stop acting between the mobile frame and slider A. The ratchet disengagement is obtained by direct contact between cursor A and the ratchet itself.

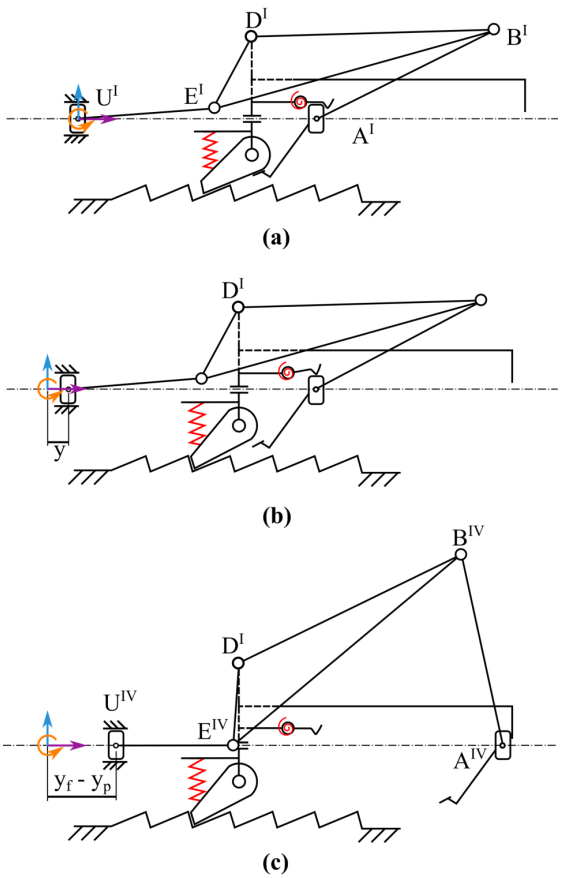

FIGURE 13: EPB.QI with flat springs and ratchet-based OWC in initial (a), intermediate (b) and final (c) rotation mode configuration.

4.2 Preliminary prototype and engagement validation

This subsection presents a preliminary experimental validation of what previously described regarding the EPB.QI mode transistion and the actual functioning of the mobile frame locking system[1]. The EPB.QI custom components, i.e. the linkage links and cursors, were made using the FDM (Fused Deposition Modelling) additive manufacturing method in PLA (polylactic acid) plastic, while the rest, i.e. springs, sliders, sleeves, were selected from commercial and standard components.
The trials on this first version of the EPB.QI transmission system evidenced how the reliability of the mode transition could be mainly compromised during the disengagement phase, i.e. when the EPB.QI is supposed to switch from the rotation mode to the traslation mode; thus it corresponds to the parking brake release. In this scenario, the mobile frame backward motion is prevented by the interaction between the ratchet gear rack and the pawl, but the resulting force $R_{D,O}^{mobile\,frame}(x)$ already described in Eqn. 22 may hinder the pawl release. As a result, the prototype design was slightly modified, by adding the possibility of an extra-rotation of BDE during the disengagement to diminish the pulling force F_U acting on the EPB.QI. Fig. 14 shows the two EPB.QI main configurations corresponding to $Y = Y_i$ and $Y = Y_i + y_f$ of Fig. 5. Regarding the whole EPB.QI test bench, Fig. 15 shows a 3D model of the entire system. The chosen mobile frame locking

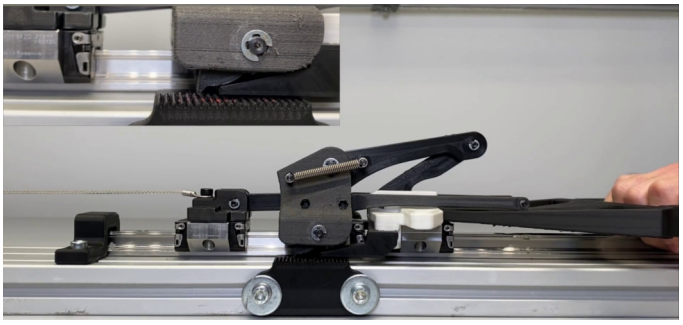

(a)

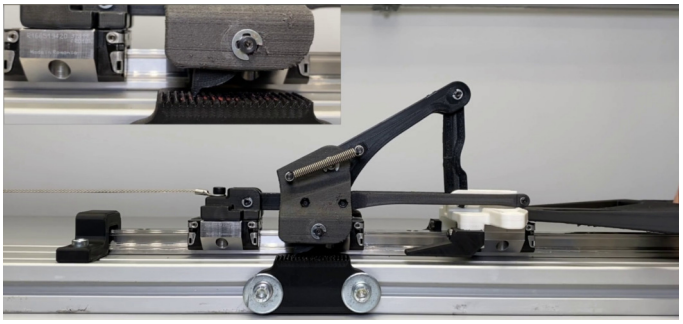

(b)

FIGURE 14: The EPB.QI planar linkage first prototype in its main configurations. A detailed view of the pawl - ratchet rack is shown in the upper left side of both sub-figures. (a) $Y = Y_i$, (b) $Y = Y_i + y_f$.

[1]The following supplementary video also shows and describes the EPB.QI planar linkage behaviour:https://youtu.be/3lObtZTqV9A

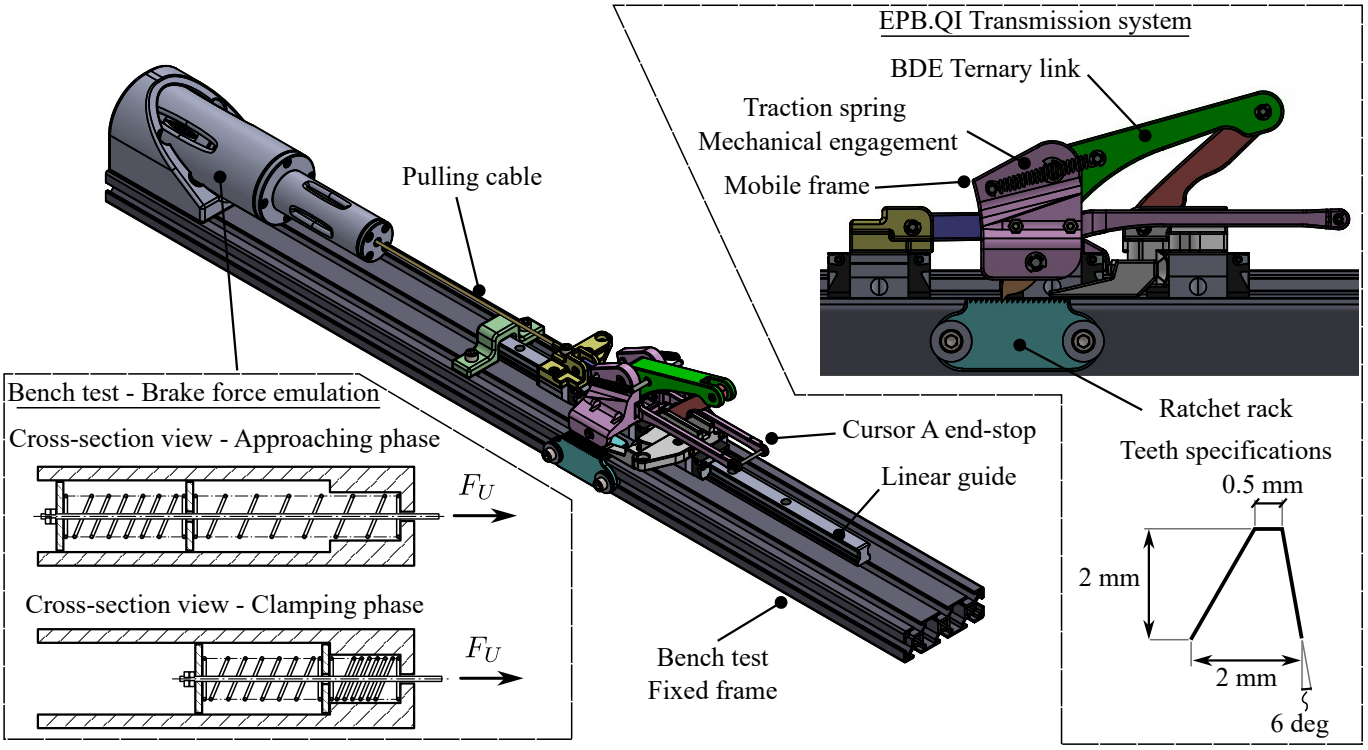

FIGURE 15: Axonometric view of the EPB.QI prototype also including the experimental test bench. The spring assebly described in the left bottom area replicate the pulling force F_U characteristics above described.

system is here composed by mechanical engagement with traction springs and a ratchet-based OWC, this latter also manufactured in FDM and characterized by a trapezoidal shape with a teeth spacing of 2 mm, an height of 2 mm, and a minimum tooth tickness of 0.5 mm. Apart from the EPB.QI prototype, the test bench includes a spring assembly composed by two compression springs to reproduce the brake force characteristics shown in Fig. 5. The two springs actually extert an elastic force respectively during the approaching and clamping phase, as it is also depicted within the Figure. The maximum value of the pulling force during the approaching phase was set to a value of $F_{U,S} = 17$ N while the maximum brake force had a value of $F_{U,M} = 150$ N

It should be noted that the system shown in Fig. 15 does not have a drive motor and not even the EPB.QI motion converter (see Fig. 2), therefore cursor A of EPB.QI was manually driven by an operator as shown in Fig. 14 (a).

The test bench has a total longitudinal encumbrance along $\hat{i}$ axis of 80 cm (from spring assembly to the end of the linear guide), a maximum heigth of 14 cm along $\hat{j}$ and it is 9 cm thick. Regarding the maximum allowed stroke of the pulling cable, the prototype was manufactured with a maximum traslation mode stroke of $Y_i = 18$ cm, but the actual value that was used was equal to $Y_i = 40$ mm. The rotation mode was instead characterized by a cable stroke value equal to $y_f = y_{f,int} = 15$ mm.

5. DRIVE MOTOR ANALYSIS

Since the EPB.QI is meant to act as both a torque amplifier and motion converter, the design procedure explained in section 3, especially in terms of the design parameter b, must guarantee the drive kinematic chain of the transmission system does not need additional gears to reach the torque required by the vehicle brake pads. This feature is clearly affected by several determinants, as for instance the pulling force characteristics explained in Fig. 5, the EPB.QI inertia and transmission ratio in Fig. 10 and the $x = x(t)$ equation of motion. Nevertheless, it is worth underlining the standard layout of a cable puller EPB converts the motion, from rotating to linear, downstream of the gearbox unit (Fig. 2), which provokes an axial tension on the screw that is comparable to the brake force F_U magnitude. In a reverse fashion, the EPB.QI drive motor is directly connected to the lead screw, thus admitting a lower screw nominal diameter thus increasing the screw transmission efficiency [17].

In addition, an upper limit to the value of T, i.e. the total brake actuation time, is often imposed not only by the required performance but also by standard regulations. Thus, T must be taken into consideration when selecting the EPB drive motor.

To this aim, a drive motor evaluation method is here discussed and schematized in Fig. 16 in the s-Domain. The method cuts out the Electronic Control Unit (ECU) drive chain controller and assumes the electric motor is supplied at the maximum supply voltage of V_m, to evaluate whether its characteristics stay within its admissible values of drive current i_m. Even though it clearly simplifies the overall EPB dynamic response, the method allows the drive motor selection among the available commercial solutions, thus postponing the ECU controller design to a subsequent and further step [12].

Table 3 resumes the input and output values of the model, categorized into three main sub-units. The screw-nut transmission effi-

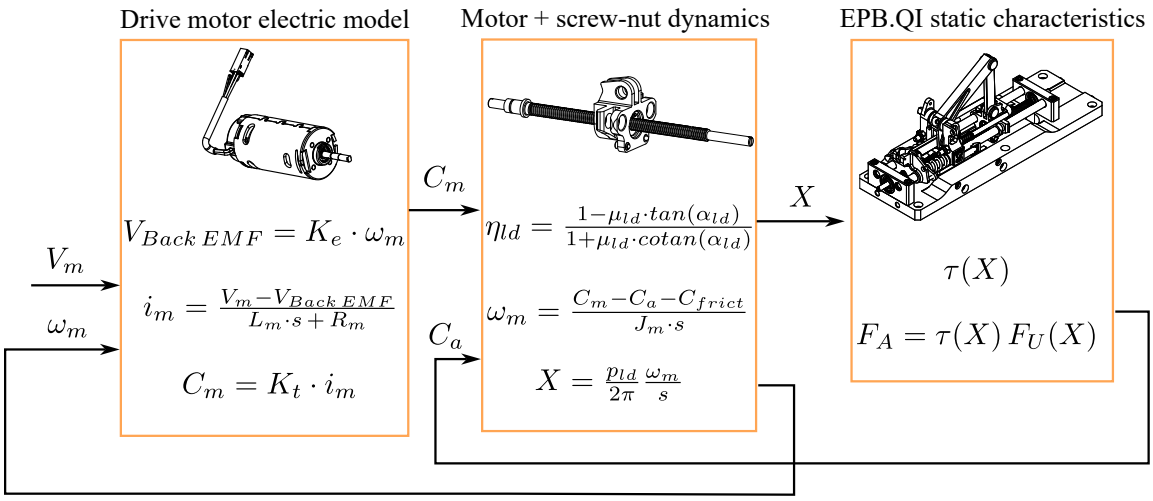

FIGURE 16: Drive chain analysis methodology. The supply voltage V_m is kept constant, thus neglecting the ECU.

ciency η_{ld} is here evaluated accordingly with [18], while C_{frict} is the resistive friction torque acting on the coupling. It is worth noticing the $F_U(X)$ characteristics is imposed by the brake system, and also the EPB.QI functional design procedure leads to the static characteristics $\tau(X)$. Besides, the supply voltage V_m is often imposed by vehicle electrical supply system combined with the electrical motor driver [2]. The present evaluation was done by considering a value of $V_m = 12$ V. The remaining free parameters of the model are thus α_{ld}, μ_{ld} and p_{ld}, regarding the lead screw, and K_e, L_m, R_m and K_t regarding the drive motor. Please notice J_m estimation can be straightforwardly done by once the EPB.QI longitudinal length along $\hat{i}$ is defined and p_{ld}, α_{ld} are known:

$$d_{ld} = \frac{p_{ld}}{\pi \tan(\alpha_{ld})} \tag{23}$$

where d_{ld} is the lead screw diameter. As additional remark, the lead-screw choice may converge toward a low value of d_{ld} in order to increase the screw transmission efficiency.
In Fig. 17 the analysis results are shown by considering the Maxon EC 60 flat brushless motor [19] and a lead-screw with $p_{ld} = 2$ mm and $\alpha_{ld} \approx 4$ deg. Regarding all the remaining input parameters here not cited, please refer to Fig. 17 caption.
The results show the selected drive chain is able to complete the brake activation in a total time $T < 1$ second, while the supply current i_m stays beneath the maximum allowed value of $i_{max} = 30$ A during the brake pads clamping.

6. CONCLUSION

The paper had presented the design of EPB.QI, a novel transmission system for cable-puller electronic parking brake devices. EPB.QI consists of a motion converter and a planar two d.o.f. linkage marked by a variable transmission ratio. The EPB.QI linkage design methods had been presented, underlining how additional components, e.g. flat springs, ratchet or sprag mechanisms, play a key role to guarantee the proper EPB.QI mode transition. The linkage design was carried out on the basis of design but also technological requirements, where the entire system is decoupled as two different slider-crank mechanisms coupled by means of the ternary link BDE. The EPB.QI linkage preliminary prototyping was presented mainly to discuss the possible system drawbacks during the engagement and disengagement phase. Towards the design and realization of a final version of the EPB.QI transmission system, the EPB.QI dynamic response, togheter with a comparison among the commercial EPB and the solution here presented, may consitute a future development of the research project.
Regarding also the final integration of the EPB.QI system with the drive chain and vehicle ECU , a preliminary assessment of the EPB drive chain was developed upon a simplified drive chain dynamic model, to inspect whether the entire system is able to complete the brake pads actuation respecting the maximum time and supply current design constraints.

ACKNOWLEDGMENTS

The authors would like to thank SKF Industrie for their financial and technical support and the staff of Nova Progetti Torino for their work in developing the EPB.QI executive design.

REFERENCES

[1] Schmittner, Bernhard. "Electric Parking Brake on the Way to Standard - New Trends." SAE Technical Paper 2015-01-2669. SAE International, Warrendale, PA. 2015. DOI 10.4271/2015-01-2669. Accessed 2023-10-18, URL https://www.sae.org/publications/technical-papers/content/2015-01-2669/. ISSN: 0148-7191, 2688-3627.

[2] Leiter, Ralf. "Design and Control of an Electric Park Brake." SAE Technical Paper 2002-01-2583. SAE International, Warrendale, PA. 2002. DOI 10.4271/2002-01-2583. Accessed 2023-10-18, URL https://www.sae.org/publications/technical-papers/content/2002-01-2583/. ISSN: 0148-7191, 2688-3627.

[3] Huang, Chien-Tai, Chen, Chien-Tzu, Cheng, Shou-Yi, Chen, Bo-Ruei and Huang, Ming-Hu. "Design and Testing of a New Electric Parking Brake Actuator." *SAE International Journal of Passenger*

TABLE 3: Input and output drive chain analysis values.

	Value	Type	Description
Motor electric model	V_m	Input	Supply voltage [V]
	K_e		Back EMF constant [V·s/rad]
	L_m, R_m		Motor inductance and resistance [H], [Ω]
	K_t		Torque constant [N·m/A]
	C_m	Output	Motor torque [Nm]
Motor + leadscrew dynamics	α_{ld}, μ_{ld}	Input	Screw lead angle and friction coefficient
	p_{ld}		Screw lead [m]
	J_m		Rotor and lead screw inertia [kg·m^2]
	ω_m	Output	Motor speed [rad/s]
	X		Slider A position along $\hat{\imath}$ axis [m]
EPQ.QI	$\tau(X)$	Input	Transmission ratio (Fig. 10)
	$F_U(X)$		Pulling force characteristics [N]
	C_a	Output	Resistive torque acting on the lead screw due to F_A [Nm]

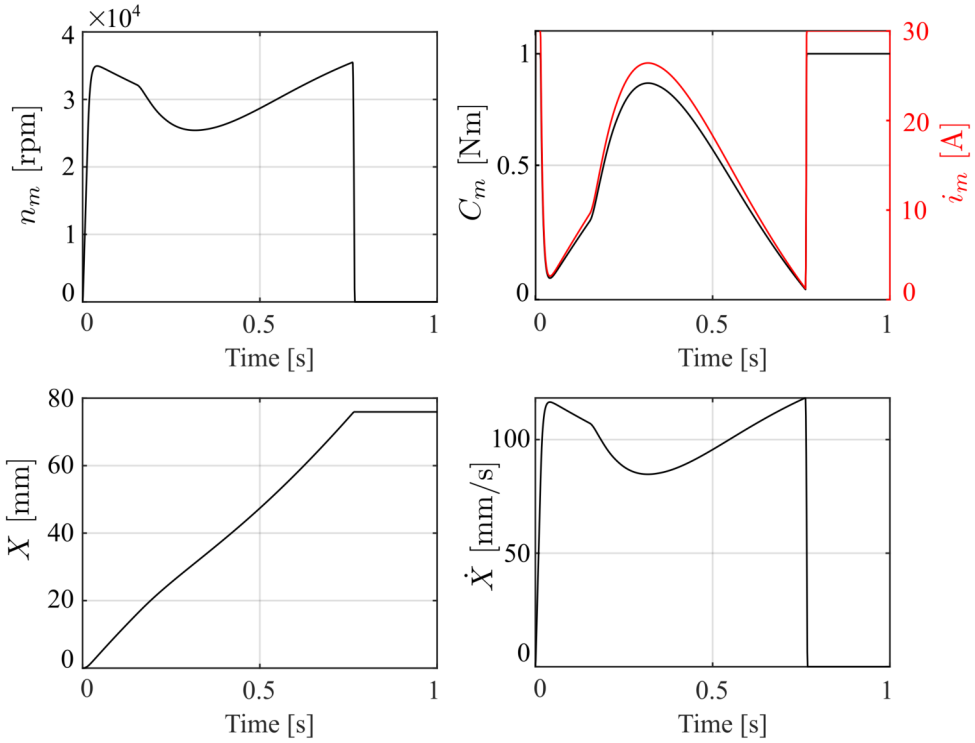

FIGURE 17: Drive chain simulation results for the Maxon EC 60 flat brushless motor, $n_m = (30/\pi) \cdot \omega_m$. The supply voltage is V_m=12 V, p_{ld}= 2 mm, $\alpha_{ld} \approx$ 4 deg. The transmission ratio is referred to the mean cable stroke $\tau(y_{f,int}$ =15 mm), while Y_i =16 mm (refer to Fig. 6). Regarding the motor drive, a maximum allowed supply current i_{max}=30 A was considered. $F_{U,S}$ = 400 N, $F_{U,M}$ = 4200 N.

Cars - Mechanical Systems Vol. 1 No. 1 (2008): pp. 1217–1222. DOI 10.4271/2008-01-2555. Accessed 2023-10-18, URL https://www.sae.org/publications/technical-papers/content/2008-01-2555/. Number: 2008-01-2555.

[4] "Parking Brake-Products and Technology | ADVICS CO.,LTD." Accessed 2023-10-18, URL https://www.advics.co.jp/eng/product/lineup/parking.html.

[5] "Continental Automotive." Accessed 2023-10-18, URL http://www.continental-automotive.com/en-gl/Passenger-Cars/Safety-and-Motion/Products/Brakes/Electronic-Brakes.

[6] "Electric Park Brake - Küster Holding GmbH." Accessed 2023-10-18, URL https://www.kuester.net/en/products/actuators/60-brake-systems/128-electric-park-brake,.

[7] "Electronic parking brake | SKF." Accessed 2023-10-18, URL https://www.skf.com/group/industries/agriculture/products-and-solutions/electronic-parking-brake.

[8] "The new Brembo's Electromechanical Braking System (EPB)." Accessed 2023-10-18, URL https://www.brembo.com/en/company/news/brembo-electromechanical-braking-system-epb.

[9] "Electric Park Brake (EPB)." Accessed 2023-10-18, URL https://www.zf.com/products/en/cars/products_64237.html.

[10] "Electric parking brake." Accessed 2023-10-18, URL https://www.hella.com/techworld/ae/Technical/Brakes/Electric-parking-brake-211/.

[11] Cheon, J. S., Jeon, J. W., Jung, H. M., Park, I. U., Park, C. H. and Yeo, T.-J. "Main Design Factors and Unified Software Structure for Cable Puller and Caliper Integrated Type Electric Parking Brakes." *SAE International Journal of Passenger Cars - Mechanical Systems* Vol. 2 No. 2 (2009): pp. 17–23. DOI 10.4271/2009-01-3022. Accessed 2023-10-18, URL https://www.sae.org/publications/technical-papers/content/2009-01-3022/. Number: 2009-01-3022.

[12] Wang, Bin, Guo, Xuexun, Zhang, Chengcai, Xiong, Zhe and Zhang, Jie. "Modeling and control of an integrated electric parking brake system." *Journal of the Franklin Institute* Vol. 352 No. 2 (2015): pp. 626–644. DOI 10.1016/j.jfranklin.2014.09.002. Accessed 2023-10-18, URL https://www.sciencedirect.com/science/article/pii/S0016003214002518.

[13] Schwarz, Ralf, Isermann, Rolf, Böhm, Jürgen, Nell, Joachim and Rieth, Peter. "Clamping Force Estimation for a Brake-by-Wire Actuator." SAE Technical Paper 1999-01-0482. SAE International, Warrendale, PA. 1999. DOI 10.4271/1999-01-0482. Accessed 2023-10-18, URL https://www.sae.org/publications/technical-papers/content/1999-01-0482/. ISSN: 0148-7191, 2688-3627.

[14] Quaglia, Giuseppe, Pepe, Fortunato and Colucci, Giovanni. "Functional Design of an Articulated Reconfigurable Mechanism for Electronic Parking Brake Systems." Laribi, Med Amine, Nelson, Carl A., Ceccarelli, Marco and Zeghloul, Saïd (eds.). *New Advances in Mechanisms, Transmissions and Applications*: pp. 306–315. 2023. Springer Nature Switzerland, Cham. DOI 10.1007/978-3-031-29815-8_30.

[15] Chesney, David R. and Kremer, John M. "Generalized Equations for Sprag One-Way Clutch Analysis and Design." *SAE Transactions* Vol. 107 (1998): pp. 1582–1592. Accessed 2023-10-16, URL https://www.jstor.org/stable/44741097. Publisher: SAE International.

[16] Bondaletov, V. P., Medvedev, V. I. and Petrov, A. V. "Reliability of free-wheel mechanisms in pulsed continuously variable transmission." *Russian Engineering Research* Vol. 30 No. 10 (2010): pp. 995–998. DOI 10.3103/S1068798X10100059. Accessed 2023-10-16, URL https://doi.org/10.3103/S1068798X10100059.

[17] Hollerbach, John M., Hunter, Ian W. and Ballantyne, John. "A comparative analysis of actuator technologies for robotics." *The robotics review 2*. MIT Press, Cambridge, MA, USA (1992): pp. 299–342.

[18] Hollander, Kevin W. and Sugar, Thomas G. "Design of Lightweight Lead Screw Actuators for Wearable Robotic Applications." *Journal of Mechanical Design* Vol. 128 No. 3 (2005): pp. 644–648. DOI 10.1115/1.2181995. Accessed 2023-10-17, URL https://doi.org/10.1115/1.2181995.

[19] "EC 60 flat with MILE Encoder and Protection Class IP 54." (2012). Accessed 2023-10-17, URL http://www.maxongroup.com/maxon/view/news/MEDIENMITTEILUNG-EC60-flat-MILE-EN.